Sensors and Materials, Vol. 12, No. 5 (2000) 301–314
MYU Tokyo

S & M 0411

Electrostatic Servo Controlled Uncooled Infrared Sensor with Tunneling Transducer

Seung Seoup Lee, Takahito Ono, Kazuhiro Nakamura and Masayoshi Esashi

Faculty of Engineering, Tohoku University
New Industry Creation Hatchery Center, Tohoku University
01 Aza Aoba, Aramaki, Aoba-ku, Sendai 980-8579, Japan

(Received July 21, 2000; accepted September 8, 2000)

Key words: infrared, bimetal, uncooled, electrostatic control, tunneling current

An uncooled infrared sensor is fabricated with the structure of a bimetallic cantilever. A NiCr(80:20) film is formed on the cantilever. The NiCr film absorbs infrared radiation and causes the cantilever to bend by the thermal bimetallic effect. In this device, a tunneling current displacement transducer is employed to detect the deflection of the bimetallic structure. The detection is achieved by electrostatic servo feedback control and the tunneling gap is kept contant during the infrared irradiation. The absorbed infrared is measured by the feedback signal. In this paper, not only the sensor performance and feedback control but also basic characteristics such as electrostatic actuation and bimetallic displacement due to infrared absorption are estimated and discussed.

1. Introduction

Infrared (IR) imagers have attracted attention for various military applications as well as commercial night vision, fire alarms and medical applications. Mechanisms to detect infrared radiation can be classified into two groups: photon detection and thermal detection. In the evolution of modern infrared detection systems, photon detectors play a major role due to their fast response time and high sensitivity.[1] However, photon detectors are too expensive for general commercial applications. Recently, with the advent of the focal plane array (FPA) concept, uncooled thermal detectors began to be

used in thermal imaging systems because they do not need a fast response for the 2D array. Uncooled IR sensors are generally based on the thermal detection principle. In thermal sensors, infrared radiation is captured by an absorber, converted to heat, and detected by a thermometer. By measuring the temperature of the thermometer, it is possible to determine the flux of incoming IR radiation. In the design of thermal detectors, the sensitivity to infrared is optimized by increasing the absorber efficiency and the thermometer sensitivity. The responsivity is enhanced by minimizing the heat capacity of sensing elements. To meet these performance criteria, the microsized infrared detector is required.

In this paper, we propose a highly sensitive thermal infrared sensor using a tunneling current displacement transducer and an electrostatic servo control. Rockstad *et al.* developed a tunneling accelerometer[2] fabricated by silicon micromachining in which a narrow tunneling gap with a gold-coated tip is used as a tunneling based displacement transducer. Uncooled infrared sensors of the Golay Cell type were also developed.[3] Basically these mechanical infrared sensors utilize a thermo-mechanical displacement induced by infrared absorption. The displacement can be measured by many kinds of displacement transducers, using lasers, piezoresistors and capacitors. For instance, Manalis *et al.* developed a two-dimensional micromechanical bimorph array for detection of thermal radiation using a laser detection transducer,[4] and Amantea *et al.* developed an uncooled IR imager with a 5 mK noise equivalent temperature difference (NEDT) using a capacitance detection transducer.[5] Each method using these transducers has its own disadvantages in terms of measuring infrared. In the case of the laser displacement transducer, heating by the asorption of laser light raises the temperature of the sensor element, which results in increasing thermomechanical noise. For piezoresistive transducers, current flow raises the temperature of the sensor elements as well. However, the capacitive transducer and the tunneling transducer are advantageous for minimizing the heat generated in the displacement measurement. Furthermore, the highest resolution for displacement is expected for a tunneling transducer. In this paper, we present a newly developed bimetallic cantilever infrared sensor based on tunneling displacement measurements. The design concept of the micro-infrared sensor, details of the fabrication process, some issues in the fabrication process and the measurement of sensor characteristics are presented. The basic characteristics such as electrostatic actuation and the bimetallic displacement due to infrared radiation are presented. The sensitivity and the noise characteristics, such as the 1/f noise of the sensor, are also discussed.

2. Structure and Operational Principles

An IR sensor is fabricated by silicon bulk micromachining techniques. A schematic diagram of the sensor is shown in Fig. 1. The device consists of three parts: a photothermal sensor having a bimetallic cantilever structure, a tunneling current-based displacement transducer with a narrow tunneling gap to detect the displacement of the bimetallic cantilever, and electrostatic feedback electrodes to hold the tunneling gap constant. The photothermal sensor, i.e., the bimetallic cantilever, has a silicon cantilever on which a metal is deposited.

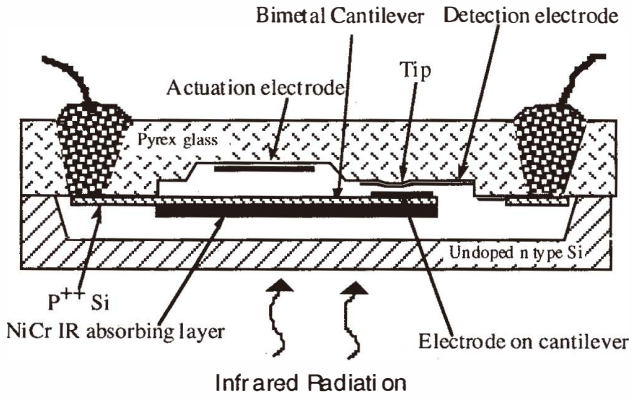

Fig. 1. Schematic diagram of IR sensor.

The thermal expansion coefficient of the metal film is larger than that of silicon. Therefore, increasing the temperature bends the cantilever. At the same time, the metal thin film acts as an absorber for IR using NiCr(80:20) film. The cantilever is formed on the glass substrate. A small displacement is measured from the change of the tunneling current between the metal electrodes formed on the glass and the cantilever. All elements of the sensor are hermetically sealed in vacuum by anodic bonding of silicon to the glass in vacuum to prevent thermal convection and to increase the sensitivity. IR radiation from the silicon side is absorbed by the absorber, which results in the deflection of the cantilever. The device is operated under electrostatic feedback control to hold the tunneling current constant by applying a servo voltage to an actuation electrode. The feedback control allows the dynamic range of the IR sensor to be extended. Electrical feedthrough is formed in the glass. The gap for electrostatic actuation is designed to be 6 μm, and the tunneling gap for detection is 1.5 μm.

In electrostatic actuation, it is known that the actuation range is limited by a pull-in voltage. At this critical point, the cantilever cannot withstand the attractive electrostatic force because the stored electrostatic energy exceeds the stored elastic energy in the cantilever and 'snaps' into the counter-electrode. The distance that the cantilever snaps toward the counter-electrode is called the snapping distance. Generally the snapping distance is one-third of the initial gap.[6] By designing the gap to be 6 μm, the snap distance is expected to be 2 μm. A bimetallic cantilever can produce a large displacement and is robust.[7] The displacement generated in the bimetallic cantilever is caused by the different thermal expansion coefficients.

In this device, the NiCr(80:20) layer with a large thermal expansion coefficient (17 ppm/°C) is deposited on the Si cantilever with a low thermal expansion coefficient (2.3 ppm/°C). The bimetallic deflection Δd at the free end of the cantilever can be expressed as follows:[8]

$$\Delta d = \left[\left(\frac{3x^2}{8t_1}\right)(\alpha_1 - \alpha_2)\right](T - T_0)\left[\frac{8(1+m)}{4+6m+4m^2+nm^3+\frac{1}{nm}}\right], \quad (1)$$

where χ is the length of the cantilever, α is the thermal expansion coefficient, t_1 is the thickness of the material with the larger thermal expansion coefficient, T is the temperature, T_0 is the reference temperature, m is the thicknesses ratio of the two materials ($t_{2,Si}/t_{1,NiCr}$), and n is the ratio of the Young's moduli of the two materials ($E_{2,Si}/E_{1,NiCr}$). (Refer to Fig. 2 for other parameters) The thickness ratio (m) of the bimetallic layers and the cantilever length should be designed to achieve the desired bimetallic deflection according to a temperature change. The deflection of the cantilever is calculated from eq. (1) as a function of the thickness ratio (m) of the bimetallic layers as shown in Fig. 3. In this calculation, the length of the cantilever and the temperature change are defined as L=450 μm and ΔT=1°C, respectively. From Fig. 3, we can see the cantilever deflection has a maximum value as the thickness ratio changes. It can also be seen that the deflection largely depends on the thickness. This is a key factor to determine the sensitivity of the sensor. However, in this device, as for the actual thickness ratio, only from 5 to 10 is used, even though a maximum deflection can be achieved with a thickness ratio of less than one ($t_{Si}/t_{NiCr} < 1$), because of the difficulty of controlling film stress which influences the initial bending. We can see the expected sensitivity of the sensor is about 0.11 μm/°C from the above calculation when the designed thickness ratio (t_{Si}/t_{NiCr}) is 10 (in the case, t_{NiCr} is 0.6 μm).

To achieve the maximum sensitivity of a thermal infrared sensor, the inicident radiation must be efficiently absorbed. The absorbing layer is used to transform the infrared radiation into heat. A high absorptivity, small heat capacity, and compatibility with mass production of the absorbing layer are also required. Generally as an IR absorbing layer, metal black such as gold black or platium black is used. However, as an

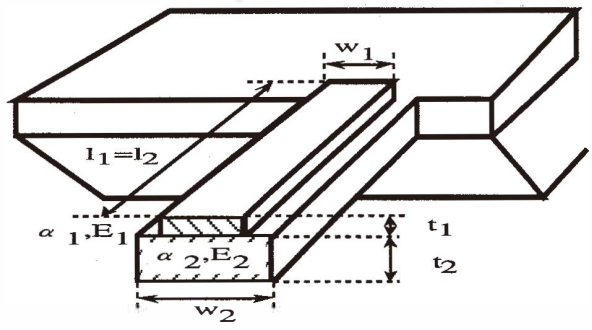

Fig. 2. Schematic illustration of a bimetallic cantilever.

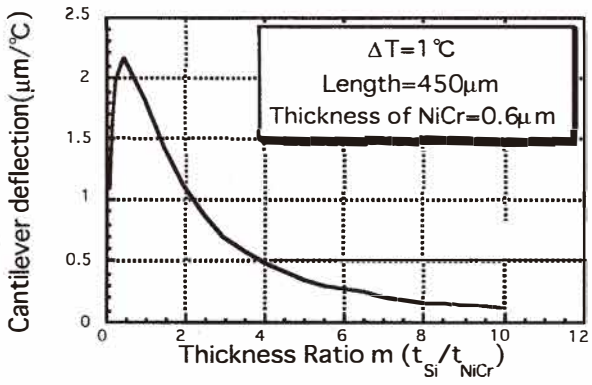

Fig. 3. Calculated cantilever deflection vs bimetal thickness ratio m (t_{Si}/t_{NiCr}).

actual absorbing layer, metal black has drawbacks due to its weak adhesion and fragility.[9] For these reasons, instead of metal black, NiCr(80:20) metal film (>2000 Å) is adopted in spite of its lower absorptivity compared with metal black layers from mid-infrared to far-infrared (3 μm–15 μm). One of the merits of a NiCr absorbing layer is that the NiCr film can be used as a bimetallic film at the same time.

We use electrostatic actuation to control the position of the cantilever. When the free end of the cantilever approaches the counter-electrode, the tunneling current generated between a pair of electrodes is expressed as follows:[6,10]

$$I = V \exp(-\alpha\sqrt{\phi}s), \tag{2}$$

where ϕ is the effective height of the tunneling barrier, s is the distance between two electrodes, V is the bias voltage (small compared with ϕ), and α is 1.025 ($\text{Å}^{-1}\text{eV}^{-1/2}$). From eq. (2), we can see the tunneling current varies exponentially according to the bending of the cantilever. Therefore, we can see the tunneling transducers have an extremely high sensitivity to displacement.

To keep the tunneling current constant, the gap between the electrodes must be controlled precisely by electrostatic forces. By monitoring the feedback signals produced by the control circuit, we can detect the change in displacement. Figure 4 shows a schematic diagram of the feedback control system for the device. It allows the measurement of small deflections with this simple circuit.

First, the measured tunneling current is converted to a voltage by a low noise current preamplifier (I/V converter). For the tunneling, a 100 mV tunneling bias is applied to the cantilever, and the preamplifier (I/V converter) gain is set to 10^7 V/A. Its output voltage from the I/V converter is compared with a reference voltage (V_{ref}) from a differential operational amplifier, generating an error signal. The reference voltage determines the amount of tunneling current. The resulting feedback signal is amplified by a high voltage booster amplifier and then applied to the actuation electrode on the glass.

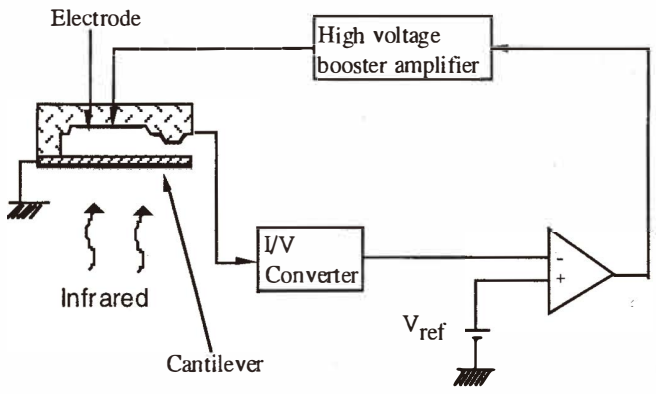

Fig. 4. A schematic diagram of the measurement system.

3. Fabrication

The structure is fabricated by a silicon micromachining technique as illustrated in Fig. 5. Pyrex glass (1 mm thick) is etched by buffered hydrofluoric acid (BHF) three times to form the tip and a step (a, b). Pt/Ti is deposited to form both the actuation electrode and the detection electrode on the Pyrex glass by sputtering and then is patterned by lift-off (c, d). As for the silicon, only one side of the Si wafer is highly boron-doped to a depth of 5 μm (e, f). After boron diffusion, Pt/Ti is deposited on the wafer by sputtering, and the electrode is produced on the cantilever by lift-off (f). The anodic bonding between the Pyrex glass and the silicon wafer is carried out at 370°C in a vacuum chamber (g). Silicon is etched in a solution of ethylene, diaminepyrocatechol and water (EPW) until a p++ Si diaphragm (5 μm thick) remained as a result of an etch stop mechanism called the lost wafer process (h). The bimetallic layer (0.6 μm thick) of NiCr is deposited by RF magnetron sputtering (i). The absorptivity of the deposited NiCr (500 nm thick) measured by Fourier transform infrared spectroscopy (FT-IR) was about 93% in the mid-to-far infrared range. The residual thermal stress of the NiCr bimetallic layer is one of the key factors in controlling the initial bending of the cantilever. Therefore, it is necessary to optimize the NiCr film stress to keep the tunneling gap narrow. We had measured the change in film stress under various sputtering conditions. As a result, we found that the Ar pressure during sputtering is one of the important factors to control the NiCr film stress. The measured NiCr film stress vs Ar pressure is plotted in Fig. 6. We must also be careful about the stress of the boron diffused layer, because a Si wafer would be stressed by the diffusion of boron atoms. Therefore, NiCr is deposited under conditions to minimize the bending of the bimetallic cantilever. After NiCr is sputtered, a Si membrane is patterned by photolithography and the cantilever is fabricated from the diaphragm by reactive ion etching (RIE) (j). Finally the sensor is packaged (k).

Figure 7 shows a SEM micrograph of a fabricated infrared sensor. The gap between the actuation electrode and the cantilever is 6 μm. The length, width and thickness of the

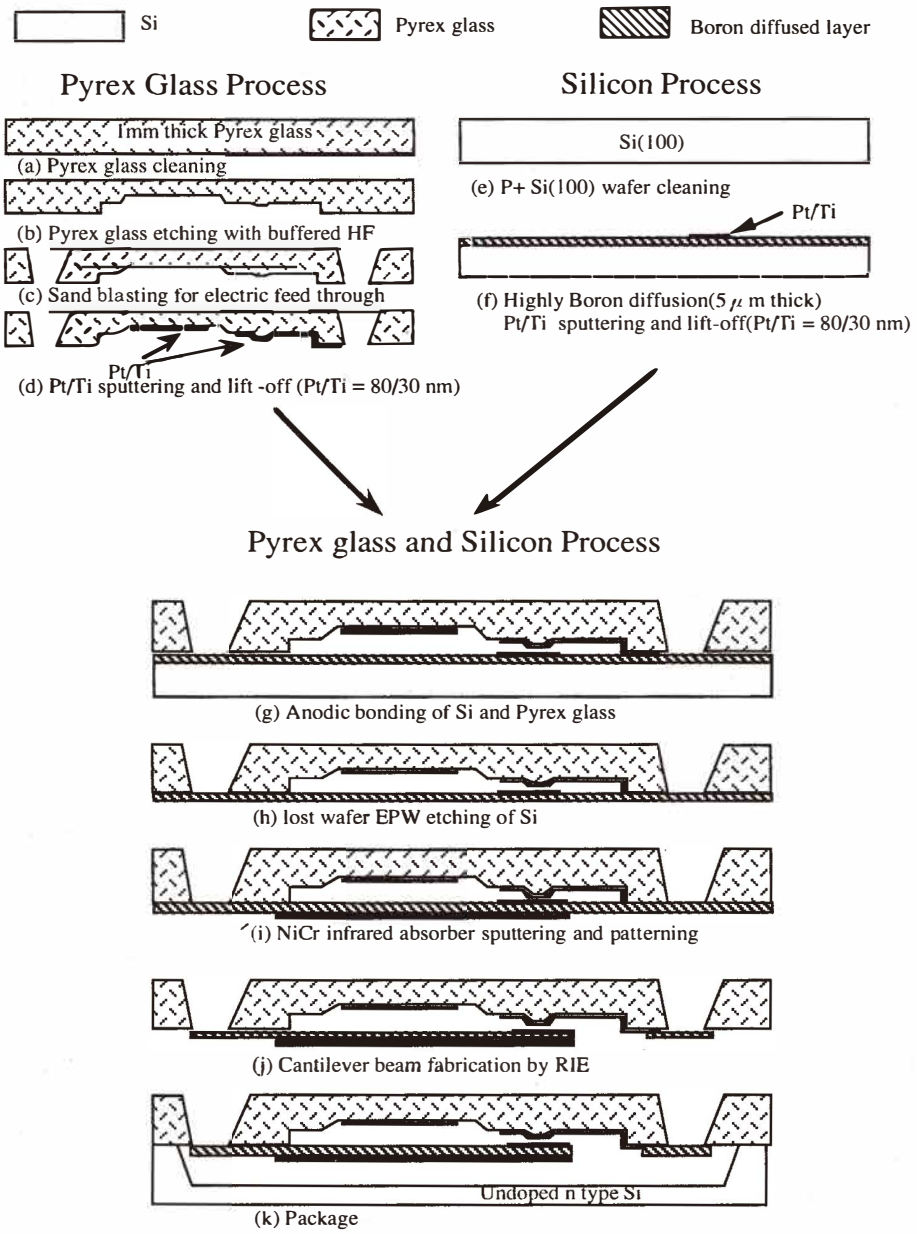

Fig. 5. Fabrication process for the infrared sensor.

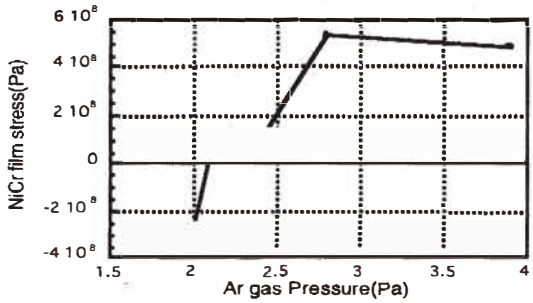

Fig. 6. NiCr film stress vs Ar gas pressure.

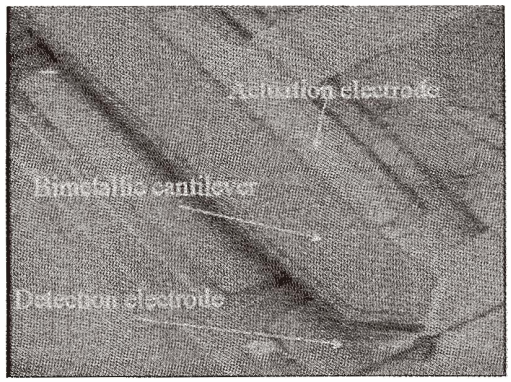

Fig. 7. Fabricated infrared sensor.

fabricated Si cantilever are 450 μm, 100 μm and 5 μm, respectively. According to the design specifications, the thickness of the Si layer should be 6 μm to yield a thickness ratio of 10 between NiCr (0.6 μm thick) and Si. In the actual fabricated device, however, the thickness of the Si layer was 5 μm due to some difficulty of boron diffusing to Si.

4. Results and Discussion

First, we measured the electrostatic actuation voltage vs displacement at three different points on the cantilever. The experimental results are shown in Fig. 8. Figure 9 shows the three points measured on the cantilever. The displacement of the cantilever is measured by a heterodyne laser displacement sensor (NEO-ARK MLD-102).

Because of the initial bending of the cantilever, the actuation gap became larger than the designed value shown in Fig. 10. The designed gap of actuation (D_a) and that of detection (D_{dd}) are 6 μm and 1.5 μm, respectively. These are designed to prevent the pull-in phenomena mentioned previously. However, the fabricated cantilever was bent by the

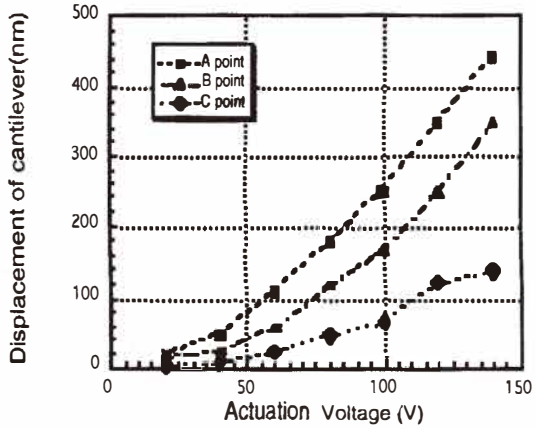

Fig. 8. Actuation voltage vs displacement of electrostatic actuation.

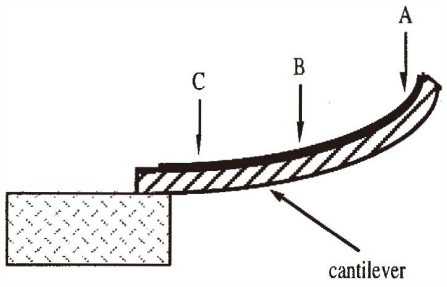

Fig. 9. Measuring points for the cantilever.

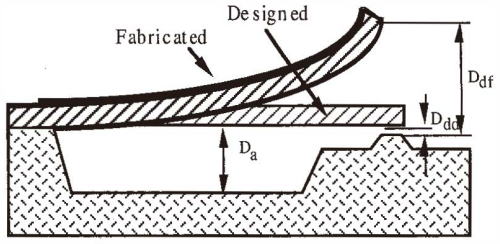

Fig. 10. The effect of the initial bending of the cantilever.

built-in stress. If the fabricated detection gap (D_{df}) is too large, the pull-in phenomena can not be prevented.

The deflection of the cantilever vs substrate temperature is shown in Fig. 11. From

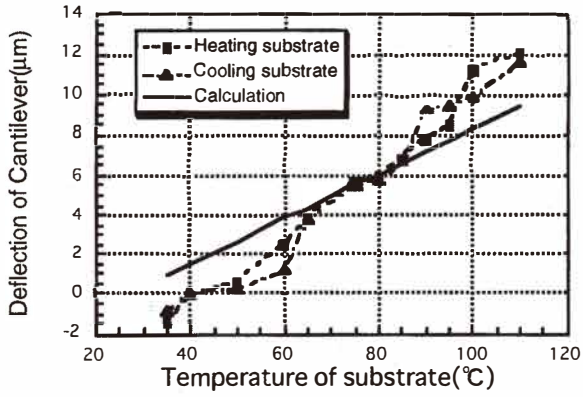

Fig. 11. Deflection of the cantilever vs temperature of substrate.

Fig. 11, we can see the deflection of the cantilever over a temperature change of 80°C is about 11 μm. It is greater than the expected value (about 9 μm displacement over a temperature change of 80°C) based on a sensitivity of 0.11 μm/°C as discussed with reference to Fig. 3. This large thermal deflection is attributed to a deposited NiCr film thicker than the designed thickness or to measurement error. The cantilever was bent initially at room temperature by the internal stress. Therefore it was not possible to measure the tunneling current at room temperature but only by the electrostatic actuation, because the gap distance was too large and the pull-in phenomena could occur before the tip of the cantilever reached the counter-electrode within the tunneling region.

To overcome this problem, we heated the sensor substrate on a hot plate to reduce the gap between the two detection electrodes. The cantilever bends by bimetallic deflection as the temperature increases. The sensor was heated to 70°C and the cantilever was pulled down by the electrostatic force until the tunneling current was measured. All experiments for tunneling current measurement were performed in air. In the experiments, the tunneling current was set to 1 nA. Next, the temperature of the sensor substrate was decreased gradually to room temperature. As the temperature decreased, the feedback voltage increased to pull down the cantilever with stronger electrostatic force while keeping the tunneling current constant. Figure 12 shows the measured feedback voltage change plotted as a function of substrate temperature. As shown in Fig. 12, the sensitivity to the temperature change is 600 mV/°C. The sensitivity over 60°C could not be measured with good reliability because of a leakage current due to ion drift in the glass substrate. Figure 13 shows the voltage noise measured using a spectrum analyzer. The small noise signal at high frequencies is attributed to the characteristics of the low-pass filter in the circuit. The source of the noise in this device has not been experimentally determined. Perhaps it may be attributed to the migration of individual platinum atoms or the migration of adsorbed water molecules through the tunneling region.[3,11]

Its sensitivity to infrared was measured by exposing the sensor to an infrared lamp with a power of 150 mW/cm^2. The measurement setup is shown in Fig. 14. Originally the

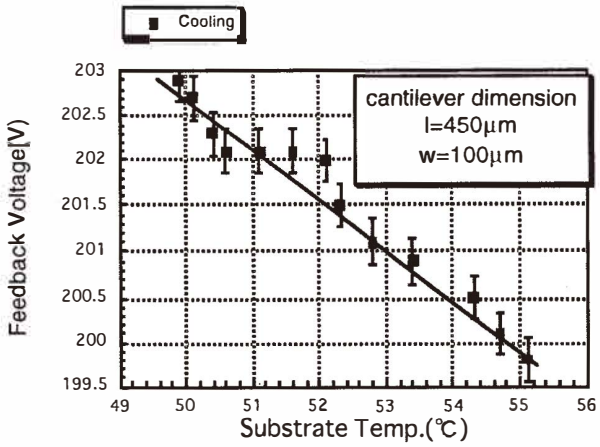

Fig. 12. Feedback voltage change plotted vs substrate temperature change.

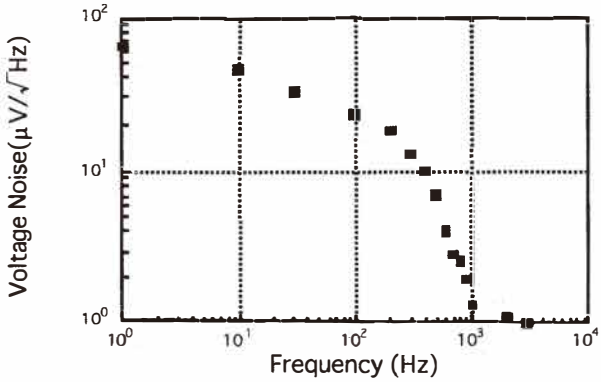

Fig. 13. Measured voltage noise at the feedback output.

device was designed with a vacuum-shielded structure for less noise (i.e., thermal noise reduction by the thermal cut) and a more stable condition. In the actual measurement, however, it was necessary to measure not only the sensor performance due to the infrared absorption but also other characteristics such as the deflection of the cantilever by the electrostatic force and the change in glass substrate temperature. Therefore, the experiment was performed without the vacuum shield, because data such as the deflection of the cantilever could not be measured using equipment like the laser Doppler in the presence of the vacuum shield. The feedback voltage change of an absorbed infrared power was 500 mV. When this was measured, the feedback voltage was in the range of 140 V to 145 V. In the electrostatic calculation, the actuation gap is supposed to be 4.9 μm from the

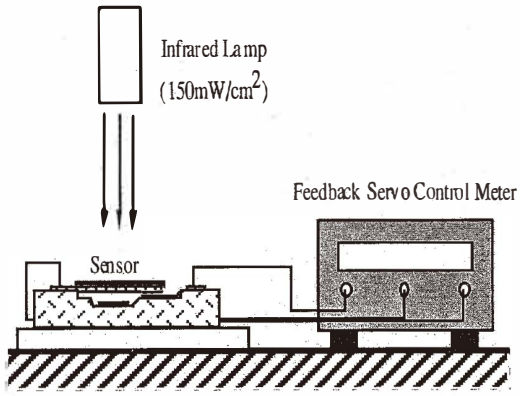

Fig. 14. Measurement setup for infrared sensing.

measurement of the laser displacement sensor. The calculated deflection as a function of applied voltage is shown in Fig. 15. It can be seen that the slope of the displacement curve is about 106 nm/V(530 Å/500 mV) in the range of the stated feedback voltage. To compare the deflection by the infrared absorption with the deflection by the electrostatic force, first it is supposed that the absorbed infrared power is uniformly distributed over the entire cantilever as shown in Fig. 16. Under this assumption, the vertical deflection of the bimetallic cantilever is calculated by the eqs. (3) and (4):[11]

$$Z = \frac{5}{4}(\alpha_1 - \alpha_2)\frac{t_1 + t_2}{t_2{}^2 K}\frac{L^3}{(\lambda_1 t_1 + \lambda_2 t_2)w}P \tag{3}$$

$$K = 4 + 6(\frac{t_1}{t_2}) + 4(\frac{t_1}{t_2})^2 + \frac{E_1}{E_2}(\frac{t_1}{t_2})^3 + \frac{E_2}{E_1}(\frac{t_2}{t_1}), \tag{4}$$

where Z is the vertical deflection of the cantilever at the end point of its length L, t is the thickness of the layers, α is the thermal expansion coefficient and λ is the thermal conductivity of the layers (λ_1 = 12.6 $WK^{-1}m^{-1}$ and λ_2 = 30 $WK^{-1}m^{-1}$) with the subscripts referring to two layers of the bimetal. That is, subscript 1 is NiCr and subscript 2 is Si. The term P is the absorbed power. If it is assumed that the actual power absorbed by NiCr is 60% by considering the heat losses by conduction toward the Pyrex glass substrate as well as air convection and also some contamination on the NiCr layer, we can achieve a deflection of 53 nm by the incident infrared power. This value coincides well with the deflection for the measured feedback voltage change. Therefore, it can be seen that the deflection corresponds to 0.001 nm/nW when an infrared power of 50.7 μW is illuminated on the sensor area. Because the noise level is measured as 35 μ V/$\sqrt{\ }$ Hz at 10 Hz, a

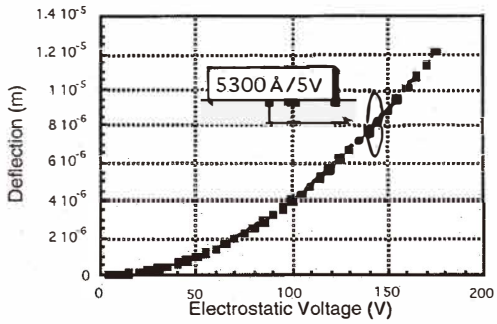

Fig. 15. The relation between electrostatic voltage and deflection.

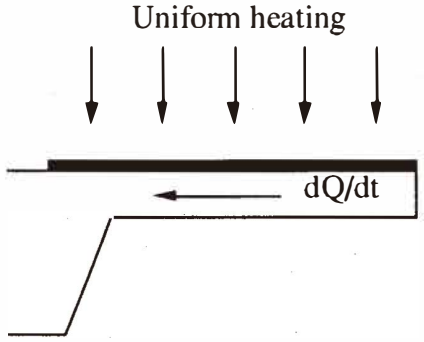

Fig. 16. Assumption for infrared absorption.

signal/noise ratio is calculated as 14. 3×3 $0\sqrt{}$ Hz at 10 Hz. Accordingly the noise equivalent power (NEP) is given as 35×10^{-10} W/$\sqrt{}$ Hz at 10 Hz and 24.4×10^{10} W/$\sqrt{}$ Hz at 30 Hz. The specific detectivity, D^*, is equal to 6.1×10^{9} cm$\sqrt{}$ Hz /W at 10 Hz and 8.7×10^{9} cm$\sqrt{}$ Hz /W at 30 Hz, where $D^* = (A^{1/2}V_{signal})/(V_{noise}P) = A^{1/2}/$ NEP, A is the area of the detector element and P is the incident optical power producing an observed signal, V_{signal}. The minimum detectable temperature difference (= ΔT/SNR) of the sensor is calculated as 58 mK. For high-performance infrared commercial sensors, D^* is on the order of 10^{8} cm$\sqrt{}$ Hz /W. The specific detectivity (on the order of 10^{6} cm$\sqrt{}$ Hz /W) of this sensor, however, is lower than that of commercial sensors at both 10 Hz and 30 Hz. These differences may be attributed to the circuit noise, the thermomechanical noise and background mechanical vibration noise among others. These noise levels can be reduced

by optimal circuit design and by a more precisely fabricated cantilever without large initial bending at room temperature.

Additionally, to see the robustness against surrounding vibrations, the resonant frequency of the sensor was measured as 34.3 kHz. Because the resonant frequency is high enough, it is expected that the external vibration does not affect the measurement of the tunneling current.

5. Conclusions

A novel infrared sensor using bimetallic displacement with tunneling current readout and electrostatic servo control is proposed, fabricated and evaluated. Feedback control by the tunneling current was successfully performed. It is expected that this sensor can have extremely high sensitivity using tunneling current readout if the signal/noise ratio is enhanced, and it shows a NEP of 35×10^{-10} W/$\sqrt{\ }$ Hz at 10 Hz for infrared irradiation.

Acknowledgments

Part of this work was carried out at VBL (Venture Business Lab.), Tohoku University. This work was supported in part by a Grant-in-Aid for Scientific Research from the Ministry of Education, Science, Sports and Culture of Japan (10305033).

References

1 P. Kruse: Infrared Technology XXI (Proc. SPIE, 1995) p. 556.
2 H. Rockstad, J. Reynolds, T. Tang, T. Kenny, W. Kaiser and T. Gabrielson: TRANSDUCERS '95 EUROSENSORS IX (1995) p. 675.
3 T. Kenny and J. Reynolds: Rev. Sci. Instrum. **67** (1996) 112.
4 S. Manalis, S. Minne and C. Quate: Appl. Phys. Lett. **70** (1997) 3311.
5 R. Amantea, L. Goodman, F. Pantuso, D. Sauer, M. Varghese, T. Villani and L. White: SPIE Aerosense '97 **3061** (1997) 210.
6 J. Brugger, N. Blanc, Ph. Renaud and N. F. de Rooij: Sensors and Actuators A **43** (1994) 339.
7 M. Hirota and S. Morita: SPIE **3436** (1998) 623.
8 J. Grade, A. Barzilai, J. Reynolds, C. Liu, A. Partridge, H. Jerman and T. Kenny: TRANSDUCERS '97 (1997) p. 1241.
9 J. Wang, P. Zavracky, N. McGruer and R. Morrison: TRANSDUCERS '97 (1997) p. 467.
10 S. Timoshenko: J. O. S. A. & R. S. I. **11** (1925) 233.
11 J. Barnes, R. Stephenson, C. Woodburn, S. O'Shea and M. Welland: Rev. Sci. Instrum. **65** (1994) 3793.